

Implications of infalling Fe II- emitting clouds in active galactic nuclei: anisotropic properties¹

Gary J. Ferland², Chen Hu³, Jian-Min Wang^{3,4}, Jack A. Baldwin⁵, Ryan L. Porter⁶, Peter A. M. van Hoof⁷ and R.J.R. Williams⁸

ABSTRACT

We investigate consequences of the discovery that Fe II emission in quasars, one of the spectroscopic signatures of “Eigenvector 1”, may originate in infalling clouds. Eigenvector 1 correlates with the Eddington ratio L/L_{Edd} so that Fe II/ H β increases as L/L_{Edd} increases. We show that the “force multiplier”, the ratio of gas opacity to electron scattering opacity, is $\sim 10^3 - 10^4$ in Fe II emitting gas. Such gas would be accelerated away from the central object if the radiation force is able to act on the entire cloud. As had previously been deduced, infall requires that the clouds have large column densities so that a substantial amount of shielded gas is present. The critical column density required for infall to occur depends on L/L_{Edd} , establishing a link between Eigenvector 1 and the Fe II/H β ratio. We see predominantly the shielded face of the infalling clouds rather than the symmetric distribution of emitters that has been assumed. The Fe II spectrum emitted by the shielded face is in good agreement with observations thus solving several long-standing mysteries in quasar emission lines.

Subject headings: accretion, accretion disks - atomic processes - galaxies: active - line: formation - quasars: emission lines

²Department of Physics, University of Kentucky, Lexington, KY 40506, USA.

³Key Laboratory for Particle Astrophysics, Institute of High Energy Physics, Chinese Academy of Sciences, Beijing 100049, China.

⁴Theoretical Physics Center for Science Facilities (TPCSF), Chinese Academy of Sciences, China.

⁵Department of Physics and Astronomy, Michigan State University, Lansing, MI, USA.

⁶Astronomy, University of Michigan, Ann Arbor, MI 48109, USA

⁷Royal Observatory of Belgium, Ringlaan 3, 1180 Brussels, Belgium

⁸AWE plc, Aldermaston, Reading RG7 4PR, UK

¹Contains material © British Crown copyright 2009/MoD.

1. Introduction

Principal component analysis (PCA) of the emission-line spectra of quasars isolates several linearly independent components (Boroson & Green 1992). These are ascribed to distinct physical processes within these objects. Eigenvector 1, which is responsible for the largest part of the variability within the samples, anti-correlates with L/L_{Edd} , the ratio of the luminosity to the Eddington limit, while Eigenvector 2 represents the accretion rate (Boroson 2002). It has been proposed that Eigenvector 1 represents the effects of radiation pressure controlling the column densities of the surviving line-emitting clouds (Marconi et al. 2008; Netzer 2009; Dong et al. 2009). This Letter is a specific, quantitative exploration of that idea.

Fe II emission is one of the main spectroscopic signatures of Eigenvector 1. The physics of Fe II emission is complex with many levels contributing to the spectrum, which occurs in a blended complex of muddled features (Wills et al. 1985, Verner et al. 1999, Baldwin et al. 2004). There has been only partial success in reproducing the observed Fe II emission in a realistic model of AGN emission-line regions (Baldwin et al. 2004).

Gaskell (2009) has recently discussed the considerable range of existing observational evidence indicating that QSO emission-line regions include infalling gas. Hu et al. (2008a) and Hu et al. (2008b) recently found that Fe II emission is systematically redshifted relative to the QSO systemic velocities, and presented the reasons suggesting that this is because the Fe II emission comes from infalling clouds. In a forthcoming paper (C. Hu et al. 2009, in preparation), we will further develop a model outlined by Hu et al. (2008b) in which the Fe II emission comes from infalling clouds systematically viewed from their shielded faces. Such clouds must have a large enough column density to fall toward the black hole, despite $L/L_{Edd} \sim 10^{-1} - 1$. Here, we describe a preliminary exploration of the basic spectroscopic properties of clouds viewed from their non-illuminated sides, which is an important question in its own right independent of the exact dynamical model. If indeed the Fe II emission does come from infalling clouds, our results have major consequences for the predicted emission-line spectrum and reveal one of the underlying drivers for Eigenvector 1.

2. Observed properties of Fe II emitters

Hu et al. (2008a) and Hu et al. (2008b) find that much of the optical Fe II emission comes from a redshifted intermediate-line region. The redshift of the Fe II-emitting region inversely correlates with the L/L_{Edd} ratio as indicated by Eigenvector 1. The correlations are that, as the L/L_{Edd} ratio increases, Fe II/ H β increases (Boroson 2002, Boroson & Green 1992) and the Fe II redshift relative to the systemic rest frame decreases (Hu et al. 2008b). These relations are the subject of

this Letter.

For simplicity, we consider two Fe II emission bands. The optical Fe II $\lambda 4558$ band is the integrated Fe II emission between $\lambda 4434$ and $\lambda 4684$, as defined by Francis et al. (1992). UV Fe II emission forms a blended pseudo continuum with very few isolated Fe II lines. We follow the Baldwin et al. (2004) definition of UV Fe II $\lambda 2445$ as the integrated Fe II flux over the wavelength range $\lambda \lambda 2240 - 2650$.

We consider the properties of a typical Fe II-emitting cloud. The observed spectrum is actually produced by a mix of clouds with a broad range of densities and distances from the central object (Baldwin et al. 1995). However, in this preliminary investigation, we consider only a single cloud.

We use a combination of line-continuum reverberation studies and theoretical predictions to determine the parameters of this typical cloud. Maoz et al. (1993) found that the UV Fe II lines in NGC 5548 respond to the driving continuum on a timescale similar to that of C IV $\lambda 1549$ and somewhat shorter than that of H β , but the optical Fe II lines in this object are too weak for useful reverberation measurements (Vestergaard & Peterson 2005). Kuehn et al. (2008) studied the reverberation behavior of the optical Fe II lines in Akn 120, for which there are no UV reverberation measurements but which has strong optical Fe II lines. They found that in Akn 120 the optical Fe II emission clearly does not originate in the same region as H β , and that there was some evidence of a reverberation response time of 300 days which implies an origin in a region several times further away from the central object than H β . A 300 day light-travel time corresponds to a source-cloud separation of $\sim 8 \times 10^{17}$ cm. For a general AGN spectral energy distribution (SED), the quoted luminosity of Akn 120 (10^{45} erg s $^{-1}$), and this separation, the flux of hydrogenizing photons, $\Phi(\text{H})$, at the derived position of the Fe II emission is in the neighborhood of $\Phi(\text{H}) \approx 10^{19}$ cm $^{-2}$ s $^{-1}$. From the results shown in Figure 7 of Baldwin et al. (2004), we estimate the gas density to be $n(\text{H}) \sim 10^{10}$ cm $^{-3}$ and the turbulence to be $u_{\text{turb}} \sim 10^2$ km s $^{-1}$. The “standard cloud” considered in the remainder of this Letter has these quantities and solar abundances.

3. Calculations

All calculations were done with version C10 of the spectral simulation code Cloudy, last described by Ferland et al. (1998). We concentrate on the emission from the shielded face of the cloud. Cloudy has long predicted the fraction of the emission that is beamed toward the central object (Ferland et al. 1992), but the outward emission, which is often quite faint for the large column densities we consider below, has not been an emphasis. The inward versus outward Fe II emission, although calculated, was not reported. We have improved the adaptive logic used to define the spatial grid to better resolve the emission from the shielded face and added several

output options to report these predictions. We now explicitly predict the inward, outward, and total Fe II emission in the form presented by Baldwin et al. (2004).

We consider the ionizing flux versus gas density plane presented by Baldwin et al. (2004). For an isotropic radiation field, the ionizing flux $\Phi(\text{H}) \propto r^{-2}$ so this variable can be thought of as a proxy for the continuum source-cloud separation. All possible AGN clouds lie somewhere on this plane. Regions with the same ionization parameter form parallel lines with a slope of unity. Little observable emission comes from the large flux, small density quadrant which corresponds to highly ionized gas with temperatures near the Compton limit (Korista et al. 1997). Clouds in the small flux, large density quadrant have very low ionization, tend to be cool, and produce strong Fe II emission.

3.1. The force multiplier

The fact that the Fe II-emitting clouds, with $L/L_{Edd} \sim 10^{-1}$, are falling into the center has major consequences for the cloud column density. The Eddington limit is the luminosity at which the force due to electron scattering balances the gravitational acceleration for optically thin gas,

$$L_{Edd} = \frac{4\pi GMm_p c}{\sigma_T}. \quad (1)$$

Here σ_T is the Thomson cross section. The ratio L/L_{Edd} is a dimensionless measurement of the specific luminosity of the AGN.

This acceleration limit is appropriate for very highly ionized gas. For gas with a higher total cross section σ , the outward force is greater by a force multiplier σ/σ_T . In general, $\sigma \gg \sigma_T$ for low-ionization gas due to the added opacity caused by line and photoelectric absorption (Castor 1974; Kippenhahn et al. 1974; Castor et al. 1975). The force multiplier over the range of densities and ionizing fluxes is shown in Figure 1, which also shows, as a shaded ellipse, the region that Baldwin et al. (2004) found could produce acceptable Fe II emission.

Figure 1 shows that typical Fe II-emitting clouds should be strongly accelerated away from the central object unless the Eddington ratio is below $L/L_{Edd} \sim 10^{-3} - 10^{-4}$. The objects in the Hu et al. (2008b) sample have $L/L_{Edd} \sim 10^{-1}$ so the gas would be expected to be accelerated outward. How can it be in a state of infall?

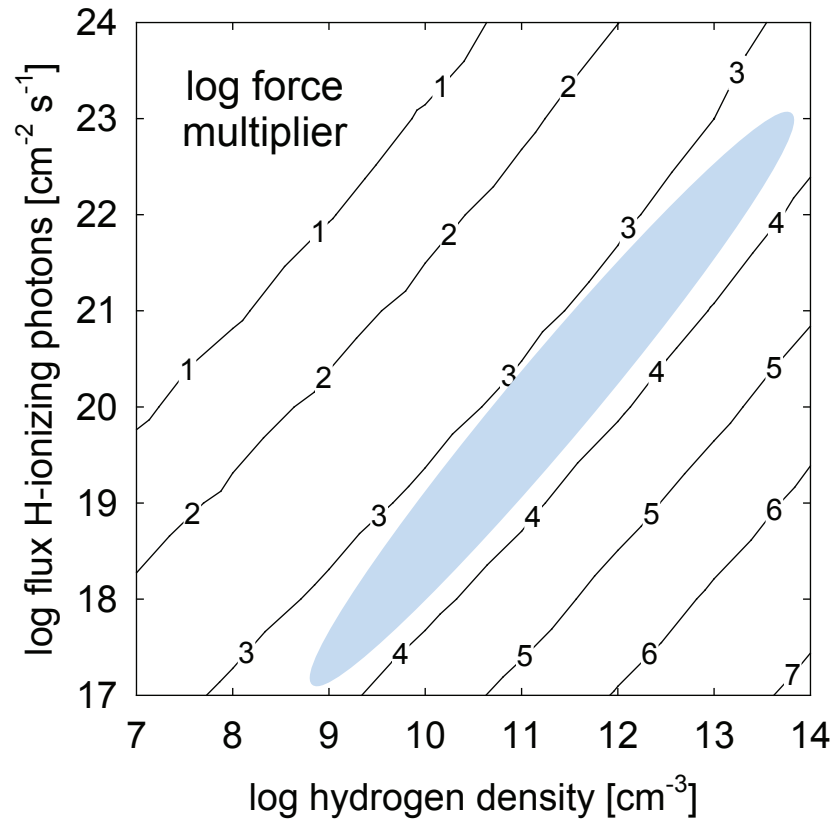


Fig. 1.— Force multiplier, evaluated at the illuminated face of the cloud, over the photon flux-density plane. The shaded ellipse is the region capable of reproducing Fe II observed emission (Baldwin et al. 2004).

3.2. The need for large column densities

The outward radiation pressure corresponding to the force multiplier shown in Figure 1 will act only on the illuminated face of a large column density cloud. This is because the peak of the SED emitted by the AGN occurs at ionizing energies. The photons most capable of pushing the gas away ionize the gas and are absorbed.

An $\text{H}^+ - \text{H}^0$ ionization front occurs when most ionizing photons have been absorbed. Most of the outward momentum acts on the H^+ layer. Relatively little energy is in high-energy photons which penetrate into neutral regions. The result is that most of the radiative acceleration occurs in the H^+ layer which then pushes on deeper neutral and molecular regions. The presence of shielded regions allows inflow to occur even at super-Eddington luminosities, as has been discussed previously (e.g., Shaviv 1998). Marconi et al. (2008) and Netzer (2009) have previously discussed radiation pressure from ionizing photons acting on large column-density AGN clouds, in terms of the effect on the deduced black hole masses and the L/L_{Edd} versus M_{BH} relation.

We quantify this with a calculation shown in Figure 2, using the standard conditions described in Section 2. The gas kinetic temperature is shown as a function of column density from the illuminated face of the cloud. A sharp drop in temperature occurs at the $\text{H}^+ - \text{H}^0$ ionization front and an H^+ layer with a column density of $N(\text{H}) \approx 5 \times 10^{21} \text{ cm}^{-2}$ exists on the face of the cloud. The vast majority of the cloud consists of warm atomic gas where the Fe II lines form.

The dashed line shows the computed radiative acceleration. Within the H^+ layer the force increases nearly linearly with increasing column density as more of the incident radiation field is absorbed. The force has nearly reached its asymptotic value when the $\text{H}^+ - \text{H}^0$ ionization front is reached. This ionized layer then pushes against the much larger column density of cooler atomic gas. The atomic layer adds mass to the cloud without contributing to its outward acceleration.

In practice, the clouds may be subject to Rayleigh-Taylor instability (Mathews 1982, Mathews 1986). While the radiation force will suppress instability at the front surface of the cloud, it will enhance the instability at the ionization front. Within the ionized region, the structure may be subject to additional radiation-driven instabilities (Mestel et al. 1976; Williams 2000), as well as significant structural perturbations due to the varying continuum. These and other sources may support a level of turbulence similar to that which we model. We will not address the stability of the clouds we model further. The model does require that the cloud integrity must be maintained by other means, possibly magnetic, or, more likely, that the cloud is an evolving dynamic entity that survives long enough to be accelerated by the gravitational forces in the region.

Figure 2 establishes the minimum column density where infall is possible. The most useful way to consider the results in Figure 2 is by reference to the acceleration that would occur for pure electron scattering opacity in fully ionized gas since that is the opacity used in the definition

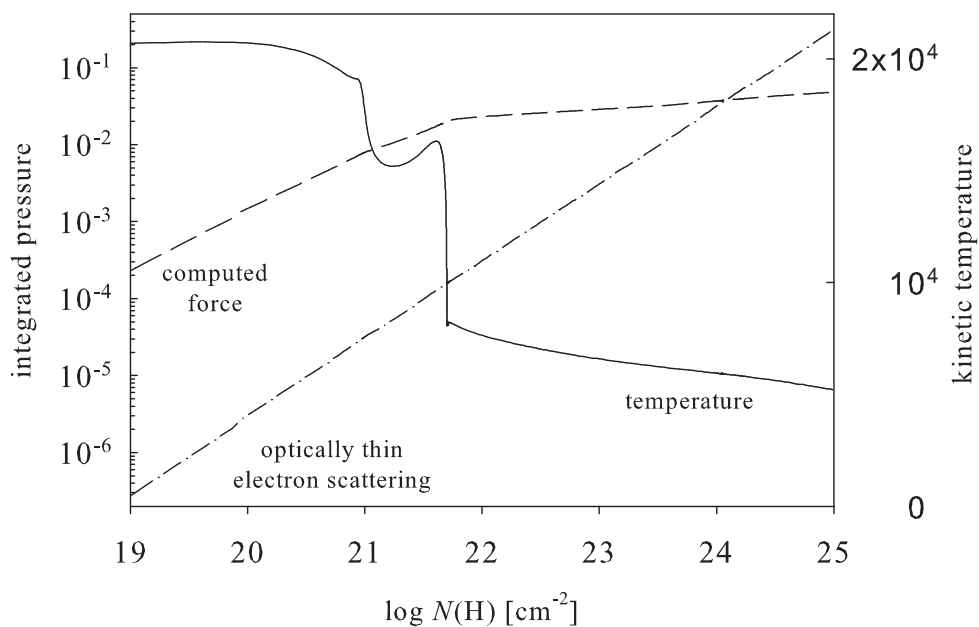


Fig. 2.— Gas kinetic temperature, the computed force for the radiative acceleration, and the force for optically thin electron scattering, are shown as a function of column density from the illuminated face. Ionizing radiation enters from the left. The two lines showing the integrated force intercept at a column density of $N(\text{H}) \approx 1.2 \times 10^{24} \text{ cm}^{-2}$, the point where the cloud would have neutral buoyancy for an AGN at the Eddington Limit.

of the Eddington limit. The dash-dotted line shows the equivalent radiative driving for the case where only electron scattering opacity acting on the incident radiation field is considered. The actual acceleration, the dashed line, is considerably larger than the electron scattering acceleration across the H^+ region, as expected from Figure 1. The acceleration increases very slowly after the $H^+ - H^0$ ionization front, while, with our definitions, the reference electron scattering acceleration increases linearly with column density $N(H)$. The two lines cross at a column density of $N(H) \approx 1.2 \times 10^{24} \text{ cm}^{-2}$, the point where the cloud would be neutrally buoyant for $L/L_{Edd} = 1$.

The minimum column density for which the inward gravitational force is stronger than the total outward radiation pressure on a cloud, $N(H)_{\text{infall}}$, may be estimated as

$$N(H)_{\text{infall}} \geq \frac{f_{\text{thick}}}{\sigma_T} \frac{L}{L_{Edd}} \simeq 1.5 \times 10^{24} f_{\text{thick}} \frac{L}{L_{Edd}} \text{ cm}^{-2}, \quad (2)$$

where $f_{\text{thick}} \sim 1$ is the fraction of the incident radiation to which the cloud is optically thick. This establishes a relation between specific luminosity and the minimal column density of infalling clouds. In objects of higher specific luminosity, which tend to have stronger Fe II emission, only high column density clouds will be able to fall inward.

Figure 3 shows how the total and, separately, the outward emission varies as the cloud column density is increased. The Fe II lines begin to form when clouds have column densities $N(H) > 10^{21.7} \text{ cm}^{-2}$, the point where the $H^+ - H^0$ ionization front occurs. This is also the column density where $H\beta$ becomes inwardly beamed. $L\alpha$ is nearly fully emitted in the inward direction (Ferland & Netzer 1979).

3.3. Isotropy of optical Fe II emission

The upper panel of Figure 4 shows the total and outward Fe II emission for our standard cloud. The spectrum is complex and it is hard to distinguish between the total and outward components in certain parts. The lower panel shows the ratio of the outward to the total emission. This shows the general trend for the inward fraction to increase with decreasing wavelength, mainly due to the larger optical depths of UV Fe II transitions.

Figure 5 compares the outward emission from our standard model with the Fe II template presented by Vestergaard & Wilkes (2001) and Boroson & Green (1992). The agreement is good. We notice in particular that the predicted optical / UV ratio, which in the simulations by Baldwin et al. (2004) is always too small when both inward and outward Fe II emission is considered, is actually larger than observed (i.e., the UV Fe II strength is underpredicted). This allows for a component of UV Fe II emission to form in the broad-line region (BLR), as suggested by reverberation results of NGC 5548 (Maoz et al. 1993).

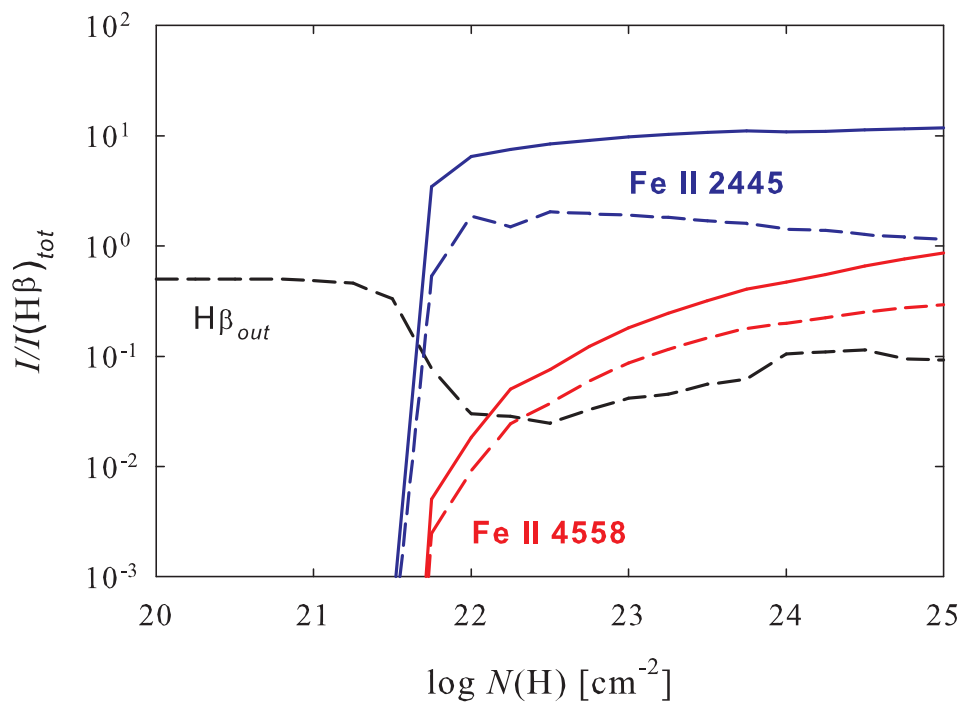


Fig. 3.— Predicted total (solid line) and outward (dashed line) emission relative to the total $\text{H}\beta$ is shown as a function of column density. $\text{H}\beta$ is isotropically emitted for small column densities while the optical Fe II band remains nearly isotropic for all column densities. The UV Fe II band is predominantly inwardly beamed due to the larger optical depth in these lines.

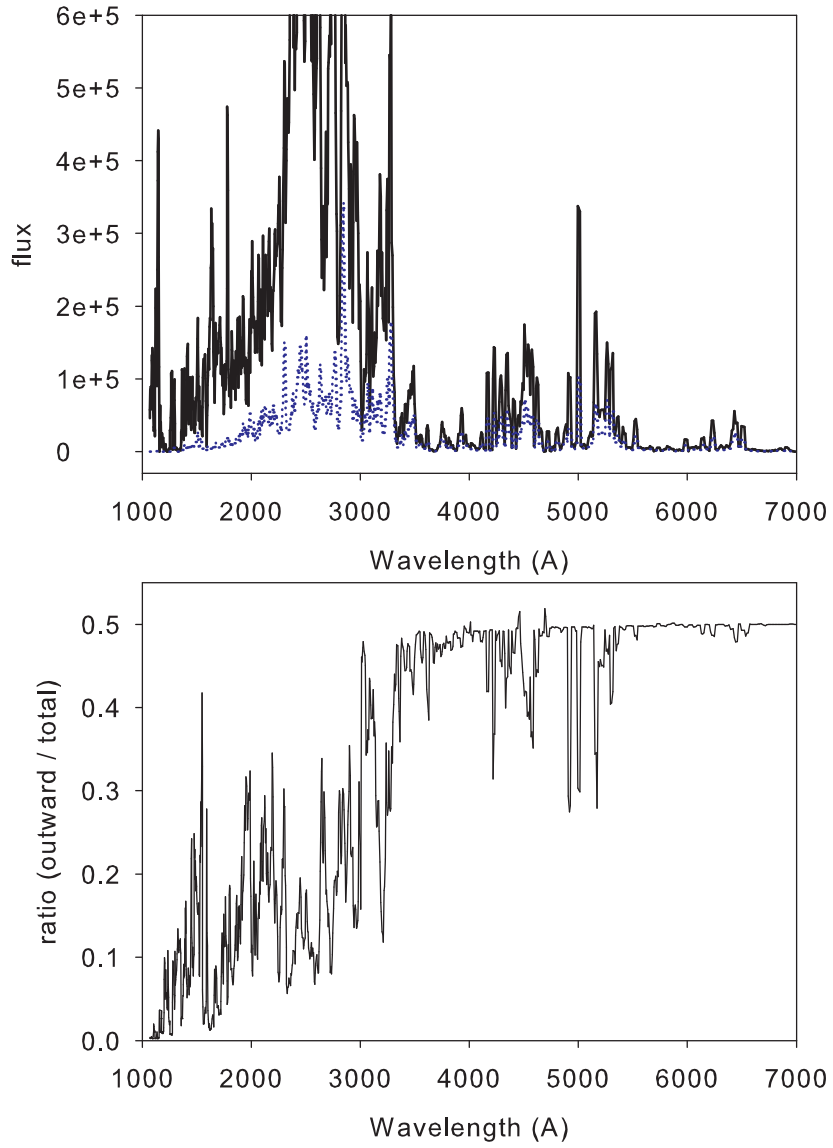


Fig. 4.— Upper panel compares the total (solid) and outward (dotted) Fe II emission of our standard cloud. The lower panel shows the ratio of the outward to total emission.

This is a major advance in the comparison between theory and observations for the Fe II emission. It is important to keep in mind the fact that the deduced properties of emission-line clouds have, until now, come from comparing the total emission, not the outward emission, with observations. Future papers will further investigate the implications of asymmetric anisotropic emission.

4. Discussion

Equation (2) suggests a linear relationship between the Eddington ratio and the column density of infalling clouds. Figure 3 shows that the Fe II/H β ratio increases with increasing column density for $N(\text{H}) \sim 10^{22} - 10^{23} \text{ cm}^{-2}$. This implies that there will be a relation between L/L_{Edd} and Fe II/H β . This explains one of the strongest systematic correlations captured by Eigenvector 1. As was also recently suggested by Dong et al. (2009), the cloud column density is the physical variant which drives the spectroscopic variations.

The predicted Fe II/H β reaches an asymptotic value of about 3 for large $N(\text{H})$ or L/L_{Edd} . This is close to the observed value for luminous quasars (Francis et al. 1991). Models which considered the full emission from the cloud do not reproduce this ratio (Baldwin et al. 2004).

L α is strongly inwardly beamed, while C IV is nearly isotropic, as shown by Ferland & Netzer (1979) and Ferland et al. (1992). Hu et al. (2008b) find that all of the emission in the optical Fe II band originates in the infalling clouds. Other lines are likely to form in both these and other regions, including the accretion disk, virialized broad-lined clouds and outflowing winds. High-resolution UV spectra of objects in which the infalling clouds have the largest velocity shift are needed to test this.

The infalling clouds must have a substantial covering factor. The observed H β equivalent widths of the broad and infalling components are similar (Hu et al. 2008a). The infalling clouds direct much of their H β emission away from the observer. They must have a covering factor approaching $\Omega/4\pi \sim 0.5$, consistent with an origin in the molecular torus (Hu et al. 2008b).

The net accretion rate due to these infalling clouds must be

$$\dot{M}_{\text{FeII}} > \frac{\Omega}{4\pi} 4\pi r^2 m_p (N_{\text{H}}/r) v_{\text{infall}} \simeq 17 \frac{\Omega}{2\pi} r_{18} N_{\text{H},24} v_8 M_{\odot} \text{yr}^{-1}, \quad (3)$$

where $r = 10^{18} r_{18} \text{ cm}$, $N_{\text{H}} = 10^{24} N_{\text{H},24} \text{ cm}^{-2}$, and $v = 1000 v_8 \text{ km s}^{-1}$. In this expression, the factor N_{H}/r is the mean density of the Fe II-emitting material multiplied by the minimal line-of-sight filling factor if the clouds are evenly distributed. This may be compared to the accretion rate of $1.8 L_{45} (\eta/0.01)^{-1} M_{\odot} \text{yr}^{-1}$ required to power an AGN of luminosity $L = 10^{45} L_{45} \text{ erg s}^{-1}$ with an

accretion efficiency of η , where the scaling parameters are all $\simeq 1$ for Akn 120. The mass infall rate above that required by accretion is likely to be balanced by other outflows. Nevertheless, this suggests that the infalling Fe II-emitting material constitutes a major element in the mass budget of high Eddington-ratio active nuclei.

We have investigated the effects of systematically viewing a low-ionization cloud from its shielded face. We focus on Fe II and H β because of their importance in PCA analysis. Meaningful predictions about the full spectrum will require a much broader exploration of, and probably a weighted integration over, the ionizing flux versus gas density plane. A future paper will carry out that broader exploration and address predicted strengths and profiles of such lines, and also the open question of whether this infalling component should be seen in absorption particularly at UV or X-ray wavelengths.

5. Conclusions

- Low-ionization Fe II-emitting clouds have force multipliers (the ratio of total to electron scattering opacities) that are large if the clouds are optically thin. Such clouds will be accelerated away from the central black hole if it has an Eddington ratio as large as those found in quasars, $L/L_{Edd} \sim 0.1$.
- If the Fe II-emitting clouds are *infalling*, as is suggested by their systemically positive velocity offsets (Hu et al. 2008b), they must have column densities significantly larger than previously thought if the inward pull of gravity is to offset the outward force of radiation pressure.
- There is a simple relationship between L/L_{Edd} and the minimum cloud column density required for infall. Fe II/H β also depends on cloud column density. Cloud column density is the underlying driver that couples Eigenvector 1, L/L_{Edd} , and spectroscopic variations, as was previously proposed by Dong et al. (2009).
- Previous simulations of the emitting gas have assumed a symmetric distribution of clouds so that, on average, we see the same number of clouds from their illuminated as from their shielded faces. We have investigated here the result of seeing an asymmetric distribution of emitters, so that we mainly observe Fe II emission from the shielded face of near-side infalling clouds, as is suggested by observations (Hu et al. 2008b, Gaskell 2009).
- Fe II UV emission is emitted less isotropically than optical Fe II lines. Previous work, which assumed a symmetric distribution of emitters, could not explain the larger-than-predicted ratio of optical to UV Fe II emission or the Fe II/H β ratio. The predicted emission ratios

from the shielded face are in good agreement with observations. This is a major advance in understanding the nature of Fe II emission in AGN.

- It is likely that there is a distribution of cloud column densities. If so, clouds with column densities smaller than that given in Equation (2) will be radiatively accelerated outward while those with larger column densities will fall in, with a column density cutoff depending on the AGN's luminosity. This would be the mechanism that accounts for the observed (Boroson 2002; Dong et al. 2009) coupling between L/L_{Edd} and the column density and Fe II/H β ratio. Both outflow and infall are observed in AGN. Could this also be a natural consequence of a range of $N(\text{H})$ in the surviving clouds?

We thank the referee for very helpful comments. G.J.F. thanks NSF and NASA for support (AST0607028, AST0908877, and ATFP07-0124), J.A.B. acknowledges NASA HST grant AR-10932, and C.H. and J.M.W. acknowledge support from NSFC-10733010 and 10821061, CAS-KJCX2-YW-T03, and 973 project (2009CB824800).

REFERENCES

- Baldwin, J., Ferland, G., Korista, K., & Verner, D. 1995, ApJ, 455, L119
- Baldwin, J. A., Ferland, G. J., Korista, K. T., Hamann, F., & LaCluyzé, A. 2004, ApJ, 615, 610
- Boroson, T. A. 2002, ApJ, 565, 78
- Boroson, T. A., & Green, R. F. 1992, ApJS, 80, 109
- Castor, J. I., Abbott, D. C., & Klein, R. I. 1975, ApJ, 195, 157
- Castor, J. L. 1974, MNRAS, 169, 279
- Dong, X., Wang, J., Wang, T., Wang, H., Fan, X., Zhou, H., & Yuan, W. 2009, arXiv0903.5020
- Ferland, G., & Netzer, H. 1979, ApJ, 229, 274
- Ferland, G. J., Korista, K. T., Verner, D. A., Ferguson, J. W., Kingdon, J. B., & Verner, E. M. 1998, PASP, 110, 761
- Ferland, G. J., Peterson, B. M., Horne, K., Welsh, W. F., & Nahar, S. N. 1992, ApJ, 387, 95
- Francis, P. J., Hewett, P. C., Foltz, C. B., & Chaffee, F. H. 1992, ApJ, 398, 476

- Francis, P. J., Hewett, P. C., Foltz, C. B., Chaffee, F. H., Weymann, R. J., & Morris, S. L. 1991, *ApJ*, 373, 465
- Gaskell, C. M. 2009, arXiv:0908.0386v2
- Hu, C., Wang, J.-M., Ho, L. C., Chen, Y.-M., Bian, W.-H., & Xue, S.-J. 2008a, *ApJ*, 683, L115
- Hu, C., Wang, J.-M., Ho, L. C., Chen, Y.-M., Zhang, H.-T., Bian, W.-H., & Xue, S.-J. 2008b, *ApJ*, 687, 78
- Kippenhahn, R., Perry, J. J., & Roser, H.-J. 1974, *A&A*, 34, 211
- Korista, K., Baldwin, J., Ferland, G., & Verner, D. 1997, *ApJS*, 108, 401
- Kuehn, C. A., Baldwin, J. A., Peterson, B. M., & Korista, K. T. 2008, *ApJ*, 673, 69
- Maoz, D., et al. 1993, *ApJ*, 404, 576
- Marconi, A., Axon, D., Maiolino, R., Nagao, T., Pastorini, G., Pietrini, P., Robinson, A., & Torricelli, G. 2008, *ApJ*, 678, 693
- Mathews, W. G. 1982, *ApJ*, 252, 39
- . 1986, *ApJ*, 305, 187
- Mestel, L., Moore, D. W., & Perry, J. J. 1976, *A&A*, 52, 203
- Netzer, H. 2009, *ApJ*, 695, 793
- Shaviv, N. J. 1998, *ApJ*, 494, L193
- Verner, E. M., Verner, D. A., Korista, K. T., Ferguson, J. W., Hamann, F., & Ferland, G. J. 1999, *ApJS*, 120, 101
- Vestergaard, M., & Peterson, B. M. 2005, *ApJ*, 625, 688
- Vestergaard, M., & Wilkes, B. J. 2001, *ApJS*, 134, 1
- Williams, R. J. R. 2000, *MNRAS*, 316, 803
- Wills, B. J., Netzer, H., & Wills, D. 1985, *ApJ*, 288, 94

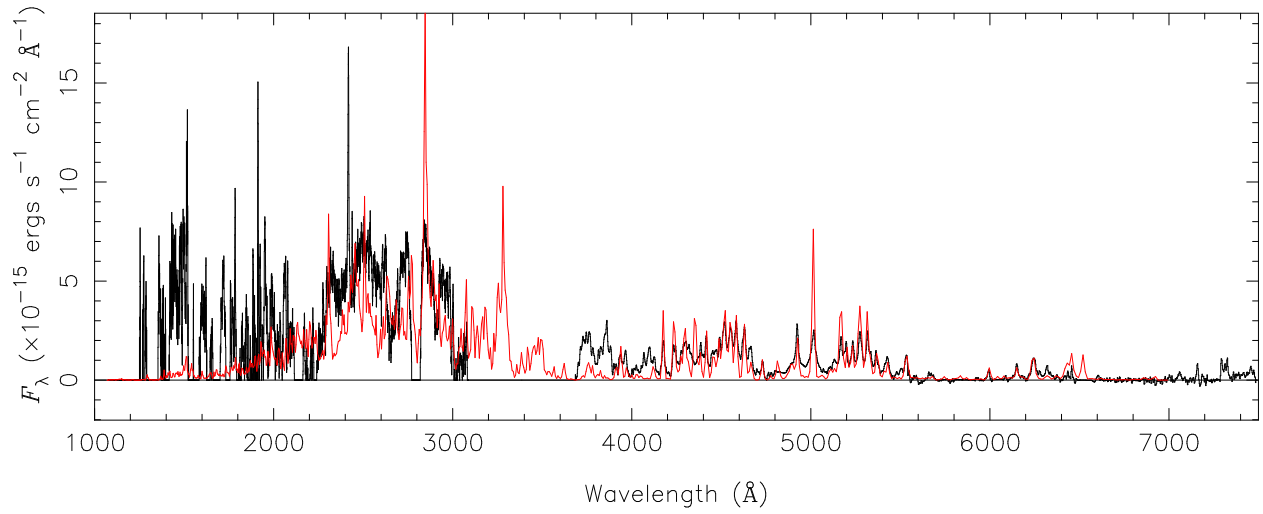


Fig. 5.— Red smoother line is the outward Fe II emission from the standard model broadened to a FWHM of 900 km s^{-1} while the black spiky line is the observed Fe II template. Intermediate-line region clouds account for the optical emission while allowing part of the UV emission to come from the inner broad-line region.